EUROPEAN FUSION DEVELOPMENT AGREEMENT

EFDA–JET–PR(04)03

D. Kalupin, M.Z. Tokar, B. Unterberg, and JET EFDA contributors

Modelling of L to H-mode Transition with the Code RITM

Modelling of L to H-mode Transition with the Code RITM

D. Kalupin[1], M.Z. Tokar[1], B. Unterberg[1],
and JET EFDA contributors*

[1] *Institut für Plasmaphysik, Forschungszentrum Jülich GmbH, EURATOM Association, D-52425 Jülich, Germany*

** See annex of J. Pamela et al, "Overview of Recent JET Results and Future Perspectives", Fusion Energy 2000 (Proc. 18th Int. Conf. Sorrento, 2000), IAEA, Vienna (2001).*

Preprint of Paper to be submitted for publication in
Plasma Physics and Controlled Fusion

ABSTRACT

The one dimensional transport code RITM was previously applied to simulate self-consistently the radial profiles of plasma parameters in the L-mode of confinement in several tokamaks. In order to describe both the L-H transition and the H-mode itself a model for Drift Alfven (DA) instability, which predicts strong reduction of DA anomalous transport at high pressure and low collisionality, has been incorporated into RITM. Additionally to the suppression of DA turbulence H-mode conditions require also that Ion Temperature Gradient (ITG) modes, which control anomalous transport in the plasma core, should be damped in the edge transport barrier. It is demonstrated that the radial density gradient, being very sharp at the plasma edge due to ionisation of recycling neutrals, plays a crucial role in damping of ITG transport in the barrier, crucially supplementing the effect of radial electric field. The results of modelling of L-H transition in JET, when the heating power exceeds a critical level, and of confinement degradation under a too strong puffing of impurities, are presented. The capability of the code RITM to reproduce the experimental scalings for the radial width of the edge pedestal is demonstrated.

1. INTRODUCTION

The High (H) confinement mode, first discovered in ASDEX-tokamak [1], was reproduced in many other fusion devices and is foreseen as a standard operational scenario for ITER [2]. The improvement of confinement in the H-mode with respect to its level in the Low (L) mode is mostly due to formation of the so-called pedestal or barrier, the region at the plasma edge characterised by extremely steep gradients of plasma parameters [1,3]. In this peripheral layer the transport of energy and particles is significantly reduced because the turbulence generated by diverse plasma instabilities is suppressed.

The most well-known approach to explain the turbulence suppression in the H-mode barrier is based on the idea that the $E\times B$ drift motion of plasma particles caused by strongly sheared radial electric field, E_r, destroys turbulent eddies [4]. On the one hand, observations on different devices, which show that after a L-H transition the E_r radial slope significantly increases in the barrier region [5], support this approach. On the other hand, E_r itself is determined by the radial gradients of plasma parameters and an ultimate answer to the question, is the increased shear of E_r the cause or result of a L-H transition, is not given yet.

Analysing the cause of transport reduction in the barrier we have to take into account the contributions from instabilities of different nature. There are specific edge instabilities, e.g., drift-Alfven (DA) or drift resistive ballooning (DRB) modes, which are maintained by coulomb collisions and, therefore, are severe at low temperatures. Numerical modelling of edge turbulence [6] predicts that the $E\times B$ rotation alone is not sufficient to stabilise these instabilities and low plasma collisionality and high pressure gradient are required for this. The latter factors are taken into account in an analytical model for DA turbulence developed in Refs.[7,8]. This model predicts that DA contribution to transport coefficients, being very important under L-mode conditions, reduces drastically if the

heating power exceeds a critical value. A predictive modelling of H-mode based on this model for DA turbulent transport was first performed in Refs.[9,10].

The suppression of edge turbulence is necessary but not enough for formation of the H-mode pedestal. Additionally, the drift modes, which dominate transport in the plasma core, should be damped in the barrier region. Normally it is assumed that the shear of the radial electric field is responsible for this[11]. However, as it is well established (see, e.g., [12]), in the H-mode without internal transport barriers the core turbulence is dominantly due to ion temperature gradient (ITG) instability, which develops when this gradient exceeds a critical level[13]. The latter is essentially determined by the density profile[13] and increases significantly at the plasma edge where the density gradient is very large due to ionisation of neutrals, recycling through the separatrix into the confined volume. This provides a mechanism for ITG suppression in the edge barrier, additional to the **E**×**B** rotation shear. The relative importance of both these stabilising factors, the **E**×**B** rotation shear and the density gradient, will be examined in the present paper. It is shown that only if the role of the density gradient is taken into account important experimentally observed features of L-H transition and scalings for edge barrier characteristics can be explained. This study is performed on the basis of numerical modelling of H-mode plasmas in JET by the one-dimensional transport code RITM [14]. RITM was previously applied to model the L-mode plasmas in different devices under diverse plasma conditions [14-21]. In order to describe H-mode the model of Refs.[7,8] for transport driven by DA turbulence has incorporated into RITM.

The reminder of the paper is organised as follows: the transport model of the RITM-code is described; the transition from L to H-mode modelled with the code is presented, where the critical power needed for the transition and evolution of different parameter profiles are discussed; the importance of the density gradient and radial electric field for the formation of the pedestal is examined; the influence of intense impurity puffs on the pedestal is presented; experimental scalings for the pedestal characteristics, e.g., its radial width and the temperature at the top of the pedestal are examined with the code; and, finally, our conclusions are given.

2. RITM-CODE, TRANSPORT MODEL

2.1 TRANSPORT EQUATIONS

The one dimensional transport RITM code allows to model the confined plasma region from plasma axis to separatrix and provides the dependencies of diverse plasma parameters on the effective minor radius of magnetic surfaces, r. For neutrals, which are produced by plasma recycling on divertor plates and enter the confined volume through separatrix RITM solves in a diffusive approximation a kinetic equation for the velocity distribution function f_n:

$$\frac{1}{g_1}\frac{\partial}{\partial r}(v_r f_n) = S_n - \nu_n f_n \qquad (1)$$

where v_r, S_n and n_n are the radial velocity, source density and ionisation frequency of neutral particles. The transport of electrons and impurity ions is described by continuity equations:

$$\frac{\partial n_e}{\partial t} + \frac{1}{r g_1}\frac{\partial}{\partial r}\left(r g_2 \Gamma_\perp^e\right) = S_n + \sum_Z Z S_Z \tag{2}$$

$$\frac{\partial n_Z}{\partial t} + \frac{1}{r g_1}\frac{\partial}{\partial r}\left(r g_2 \Gamma_\perp^Z\right) = S_Z \tag{3}$$

where $n_{e,Z}$ are the densities of the electrons and impurity species of the charge Z, and $S_{n,Z}$ are their source densities (all ionisation stages of He, C, O, Ne, Si and Ar can be taken into consideration).

The particle flux densities include both diffusive and convective contributions:

$$\Gamma_\perp^e = -D_\perp \frac{\partial n_e}{\partial r} + V_\perp n_e, \quad \Gamma_\perp^Z = -D_\perp^Z \frac{\partial n_Z}{\partial r} + V_\perp^Z n_Z \tag{4}$$

The densities and fluxes of the background ions are computed from the quasi-neutrality conditions:

$$n_i = n_e - \sum Z \cdot n_Z, \quad \Gamma_\perp^i = \Gamma_\perp^e - \sum Z \cdot \Gamma_\perp^Z \tag{5}$$

The Shafranov shift calculated from the Grad-Shafranov equation is used together with analytically prescribed elongation and triangularity of the magnetic surfaces in order to determine the metric coefficients $g_{1,2}$.

The electron and ion temperatures T_e and T_i are computed by solving heat transport equations:

$$\frac{3}{2}\frac{\partial n_e T_e}{\partial t} + \frac{1}{r g_1}\frac{\partial}{\partial r}\left[r g_2\left(1.5\Gamma_\perp^e T_e - \kappa_\perp^e \frac{\partial T_e}{\partial r}\right)\right] = \frac{J^2}{\sigma} + Q_{au}^e - Q_{ei} - Q_{en} - Q_{el} \tag{6}$$

$$\frac{3}{2}\frac{\partial n_\Sigma T_i}{\partial t} + \frac{1}{r g_1}\frac{\partial}{\partial r}\left[r g_2\left(1.5\Gamma_\perp^\Sigma T_i - \kappa_\perp^\Sigma \frac{\partial T_i}{\partial r}\right)\right] = Q_{au}^i + Q_{ei} + Q_{in} \tag{7}$$

where $n_\Sigma = n_i + \Sigma n_Z$, $\Gamma_\Sigma = \Gamma_i + \Sigma\Gamma_Z$ are the total ion density and their flux, $Q_{au}^{e,i}$ the electron and ion heat source due to additional heating from NBI and ICRH, whose radial profiles are taken from TRANSP calculations, Q_{ei}, Q_{en}, Q_{el} the energy losses from electrons due to coulomb collisions with ions, excitation and ionisation of neutrals and impurities, respectively, Q_{in} the energy exchange between main ions and neutrals.

The boundary conditions of Eqs.(2)-(7) at the separatrix, $r = a$, imply the e-folding lengths of parameters, which are taken from measurements.

2.2 TRANSPORT MODEL.

The present transport model in RITM takes into account the most important unstable drift modes. The corresponding contributions to the transport coefficients are determined in a mixing length approximation [13,22], $D \approx \frac{\gamma_{\max}}{k_{\perp,\max}^2}$. Here $g_{\max}$ is the maximum value of the instability linear growth rate g considered as a function of the perpendicular wave number $k_\wedge$ and $k_{\wedge,\max}$ is the $k_\wedge$-value where $g_{\max}$ is reached. The model from Refs.[7,8] for DA-induced transport takes additionally into

account the correction due to phase shift between perturbations of density and radial velocity, the so called improved mixing length approximation [13,23], $D \approx \frac{\gamma_{\max}}{k_{\perp,\max}^2} \frac{\gamma_{\max}^2}{\gamma_{\max}^2 + \omega_{r,\max}^2}$, with $w_{r,\max}$ being the magnitude of the real frequency at $k_{\wedge,\max}$.

The contributions from ITG and Dissipative Trapped Electron (DTE) modes are calculated according to the expressions [13,24]:

$$D^{ITG} = \frac{cT_e}{k_{\perp,\max}^{ITG} eB}\left[\left(-\frac{d\ln T_i}{dr} + \frac{2}{3}\frac{d\ln n_e}{dr}\right)(Z_{eff}R)^{-1} - \frac{1}{8}\left(\frac{d\ln n_e}{dr} + \frac{2}{R}\right)^2 - \frac{20}{9}\frac{1}{R^2 Z_{eff}^2}\right]^{1/2} \quad (8)$$

$$D^{DTE} = \rho_s f_{tr} \eta_e \omega_* \frac{\omega_* \nu_{eff}}{\omega_*^2 + \nu_{eff}^2} \quad (9)$$

where c is the speed of light, e the elementary charge, B the magnetic field induction, Z_{eff} the ion effective charge, R the plasma major radius, ρ_s the ion Larmor radius, f_{tr} the fraction of trapped particles, $\omega_* = \frac{cT_e k_{\perp,\max}^{DTE}}{eB}\left(-\frac{d\ln n_e}{dr}\right)$ the drift frequency, $\nu_{eff} = \nu_{ei} R/r$ the effective collision frequency of trapped electrons with ν_{ei} being the collision frequency of thermal electrons, $k_{\perp,\max}^{ITG} = 0.3/\rho_s$ and $k_{\perp,\max}^{DTE} = 1/\rho_s$. The generalisation of D^{ITG} on the case of impure plasmas with $Z_{eff} > 1$ was performed by taking into account the results of modelling of ITG instability in multi-species plasmas [25].

At the plasma edge, where the transport due to ITG and DTE modes is significantly reduced due to strong density gradient and decreasing temperature, respectively, DRB and DA instabilities become of most importance. According to Ref. [26]:

$$D^{DRB} \propto (2q\rho_e)^2 \nu_e R\left(-\frac{d\ln n_e}{dr}\right) \quad (10)$$

where q is the safety factor and ρ_e the electron Larmor radius.

The DA transport contribution is given by the relation [7,8]:

$$D^{DA} = \frac{\chi_{GB}}{\sqrt{\mu}} \bar{\bar{\chi}}_\perp(\beta_n, \nu_n). \quad (11)$$

Here $\chi_{GB} = \rho_s^2 c_s / L_p$ is the Gyro-Bohm diffusion with c_s being the ion sound velocity and $L_p = -1/(d\ln P/dr)$ the pressure e-folding length; $\mu = -k_\parallel V_{The} L_p / c_s$ with $k_\parallel \sim 1/qR$ and V_{the} thermal electron velocity; the dimensionless factor $\bar{\bar{\chi}}_\perp(\beta_n, \nu_n) = \left[\frac{(1+\beta_n^2)^3 + \nu_n^2}{1+\beta_n^2+\nu_n^{4/3}}\right]^{1/2}$ depends on parameters $\beta_n = \left(\frac{M_i}{m_e}\right)^{1/2} \frac{4\pi n_e T_e}{B^2} \frac{1}{k_\parallel L_p}$ and $\nu_n = \left(\frac{M_i}{m_e}\right)^{1/4} \frac{L_p^{1/2}}{\lambda_e k_\parallel^{1/2}}$, being the normalised plasma beta and electron collision frequency, respectively, λ_e the mean three path length. The formula (11) predicts a significant reduction of D^{DA} when β_n exceeds a critical value of $1+\nu_n^{2/3}$. In Ref. [8] this

condition has been used for an estimate of a critical edge temperature for a L-H transition.

The effective transport coefficients are assumed in the form:

$$D_{\perp}^{e} = D^{ITG} f_{tr} + D^{DTE} + D^{DRB} + D^{DA}, \tag{12}$$

$$V_{\perp}^{e} = \left[D^{ITG} f_{tr} \left(4r/3R\right) + D^{DTE}\right] \left(d \ln q / dr\right), \tag{13}$$

$$D_{\perp}^{Z} = D_{\perp}, \tag{14}$$

$$V_{\perp}^{Z} = V_{\perp}^{e} + V_{\perp}^{Z,NEO} \tag{15}$$

$$\kappa_{\perp}^{e} = 3/2 \left(D^{ITG} f_{tr} + D^{DTE} + D^{DRB} + D^{DA}\right) n_e, \tag{16}$$

$$\kappa_{\perp}^{i} = \kappa_{\perp}^{i,NEO} + 3/2 \left(D^{ITG} + D^{DRB} + D^{DA}\right) \tag{17}$$

The factor f_{tr} in the expression for $D_{\wedge}$ takes into account that most effectively ITG drift modes leads to the particle transport by stochastization of orbits of trapped electrons [27] and the corresponding contribution to the diffusivity should be proportional to the fraction of trapped particles. In the expression for the electron pinch-velocity the small factor $4r/3R$ represents a weak effect of ion driven modes on electron convection [28]. The impurity ion diffusion is assumed the same as for electrons; their pinch velocity, Eq.(15), is compound from anomalous and neo-classical contributions, and the latter is determined by the gradients of the density and temperature of background ions [29].

The non-linear dependence of transport coefficients on the plasma parameters and their radial gradients does not permit the convergence of calculations for time steps smaller than ~ 10ms. Therefore the ELM activity can not be explicitly modelled by RITM up to now. In order to take into account the effect of ELMs on transport it is assumed that the coefficients given by Eqs.(12)-(17) are increased exponentially when the normalised pressure gradient, $\alpha = 8\pi R q^2 \left(\partial P / \partial r\right) / B_T^2$, where P is the total pressure, exceeds the critical level $\alpha_c = 0.4s\left[1 + \kappa^2 \left(1 + 5\delta^2\right)\right]$[30], where s is the magnetic shear, k the elongation and d the triangularity of the 95% magnetic flux surface.

3. MODELLING OF L TO H-MODE TRANSITION.

To test the capability of the transport code to reproduce the L-H transition calculations were performed by varying the auxiliary heating power. The conditions of JET Pulse No: 53146 with magnetic field B_T= 2.4T, plasma current I_P= 2.3MA, elongation and triangularity δ=1.6 and κ= 0.45 respectively, were selected. The deuterium fuelling rate was adjusted to match the line averaged density $\bar{n}_e$=9.5*10^{19} m^{-3} and carbon sputtering coefficient was selected to reproduce experimental impurity content and radiation fraction.

Figure 1 shows the evolution of the edge normalised pressure gradient, α (△) and ion temperature at the middle of the transport barrier (○), starting from stationary L-mode conditions at total heating

power, P_{tot}, about 3.8MW and during linear increase of power until ~16MW when stationary H-mode is achieved. In the range of 8-12MW the power dependence becomes very non-linear so that a increases by a factor of 3.5. However, there is not any real bifurcation with an infinite slop of curves, the critical conditions for L-H transition can be at attributed to the state when this slope approaches the maximum, i.e., a power of 10-12MW. If we take into account that 25-30% of power are radiated from the confined volume, the obtained value for the critical power agrees well with an experimentally observed value of 8-9MW for the power, flowing through the separatrix, required for the L-H transition under selected plasma conditions.

The radial profiles of different plasma parameters taken between 0.85 and 1 of the normalised minor radius obtained with different heating power are shown in Fig.2. The modification of all parameters and transport characteristics are strongly non-linear interrelated and it is impossible to propose a simple and unique interpretation of the evolution obtained. As a probable sequence of events we can picture the following. An increase of the heating power leads to a certain rise of charged particle temperatures at the edge, the plasma collisionality drops and pressure gradient increases. This leads to reduction of the transport driven by Drift Alfven instability, which is the main channel for edge electron particle and heat losses under L-mode conditions. As a result a much steeper density gradient due to ionisation of recycling neutrals can be formed, see Fig.2c. This is in good agreement with the experimentally observed evolution of the density profile from L- to H-mode conditions [1]. This fact is of crucial importance for keeping ITG transport on a low level with increasing ion temperature gradient. Indeed, according to Eq.(8) $\chi^{ITG} \sim \sqrt{\nabla T - \nabla T_{crit}}$ where the critical value of the temperature gradient, ∇T_{crit}, at which the ITG-mode is completely suppressed, increases with increasing density gradient. Therefore χ^{ITG} is strongly reduced in the region $0.93 \le \rho \le 1.0$, where strong density gradient arises, Fig.2d. In the region between $\rho \cong 0.93$ and 0.98, where two major contributors to the edge transport, ITG and DA, are substantially damped, neoclassical transport becomes the leading contribution to χ_i, Fig. 2e. Formation of the layer with strongly reduced transport, which is often called as the edge transport barrier, leads to the further development of temperature and pressure, and finally results in the pedestal.

Relative importance of density gradient and radial electric field for edge barrier formation

In order to investigate this we have performed calculations when the ITG transport is reduced (i) by the density gradient only, (ii) by **E**×**B** rotation shear of the radial electric field only and (iii) by both effects simultaneously. The **E**×**B** rotation shear is computed as follows [31]:

$$S_{\perp} = c\frac{r}{B_{\varphi}}\left|\frac{\partial}{\partial r}\left(\frac{E_r}{r}\right)\right| \tag{18}$$

with the radial electric field E_r calculated from the radial component of the force balance for the main ions:

$$E_r = \frac{V_{\varphi}B_{\vartheta} - V_{\vartheta}B_{\varphi}}{c} + \frac{1}{en_i}\frac{\partial\left(n_i T_i\right)}{\partial r} \tag{19}$$

where $B_{\vartheta,\varphi}$ and $V_{\vartheta,\varphi}$ are the poloidal and toroidal components of the magnetic field and ion velocity. The radial profiles of the ion pressure and radial electric field are shown in Figs. 2g and 2h. It was assumed that $V_\varphi = 0$ and V_ϑ is given by neoclassical theory [29]:

$$V_\vartheta = k_{neo} \frac{c}{eB_\varphi} \frac{\partial T_i}{\partial r} \tag{20}$$

with the coefficient k_{neo} varying with the ion collisionality according to the approximate formula of Ref.[32].

Figure 3: Ion heat conductivity and temperature obtained with different assumptions for the stabilising factors for the transport driven by ITG turbulence.

By computing $S_\perp$ in the code all terms containing the second derivatives of parameters were neglected because these terms made calculations very unstable and led to poor convergence. However, this neglecting should not corrupt the results to strongly because in the region of the maximum transport reduction the gradients are also maximal and, thus, the second derivatives are close to zero.
The influence of $S_\perp$ of ITG transport has been calculated according to Ref.[4]:

$$D^{ITG}(S_\perp) = \frac{D^{ITG}(0)}{1 + (S_\perp / \gamma_{\max})^2} \tag{21}$$

where $D^{ITG}(0)$ is the transport coefficient without the effect of radial electric field given by Eq.(8). In the case (ii) the density gradient in $D^{ITG}(0)$ was put to zero.
Fig.3 shows the profiles of ion heat conductivity and temperature found for P_{tot}=*10.5MW*. One can see that the **E**×**B** rotation shear alone can not lead to formation of a pronounced barrier and the effect of the density gradient is more efficient for this. The obtained result does not mean that the electric field itself does change strongly from L- to H-mode. Due to increasing gradients of the ion density and temperature its maximum value and shear increase very strongly, as one can see in Fig. 2h, in agreement with experimental observation [5].

In the present form the code RITM does not allow to model the real time dynamics of the L-H transition, e.g., after an instantaneous increase of P_{tot} above the critical level. The cause is a strongly non-linearity of transport coefficients which does not permit the convergence of calculations for time steps smaller than ~ 10ms. Therefore the effect of self-generation of plasma poloidal rotation due to Reynolds stress and its importance for the dynamics of the edge barrier formation [33] can not be studied in our simulations yet. However, for quasi-stationary conditions considered here, Reynolds stress, probably, does play very significant role. As it was demonstrated by measurements on tokamak HT-6M [34] Reynolds stress is large only on a transient stage of 0.5ms duration and reduces practically to zero for later times when the plasma enters the H-mode.

5. MODELLING OF BACK H-L TRANSITION.

A too strong gas puffing applied in to order to increase the plasma density leads normally to a transient back transition to the L-mode [35]. The same can occur if too much impurities are seeded into the plasma with the aim to increase the edge radiation [36]. Here we present the result of modelling of the second situation. Initially the code is run till a stationary H mode plasma with the total heating power of 14MW and a line averaged density of 9.5×10^{13} cm^{-3} is established. The power flowing through separatrix, P_{sep}, is about 10MW and its reduction with respect to P_{tot} is due to radiation of intrinsic carbon impurity. Since the RITM-model allows the computations only from the axis of the plasma column to the separatrix, this radiation fraction represents the value of the core radiation only. For these conditions the edge profiles of the radiation loss density, electron temperature, ion heat conductivity and total pressure, shown in Fig.4 by solid curves, indicate a fully developed edge pedestal.

With the beginning of argon injection the radiation losses steady increase and saturate at a level depending on the argon puffing rate. For the rates of 2×10^{20} Ar atoms per second, typical for experiments with argon seeding into JET H-mode [37], this level is of 50%. In this case the presence of puffed impurity does not lead to any significant deterioration of confinement (see broken curves with long segments in Fig.4) in agreement with observations. When, however the intensity of the puff increases by a factor of 5 and the power radiated from the confined volume reaches a value of 70% from the total heating power, the pedestal is destroyed, as it is demonstrated by broken curves with short segments in Fig.4. While the radiation, localised mostly at the plasma edge, increases with intensification of argon puff, plasma periphery gets colder, this leads to the increase of the transport driven by DA turbulence. Enhanced DA transport flattens the density profile that leads to the resumption of ITG turbulence in the edge region and further enhancement of the edge transport. The transport barrier formed under H-mode conditions disappears.

6. SCALINGS FOR PEDESTAL CHARACTERISTICS.

The characteristics of the edge pedestal, e.g., its width and the temperatures at the pedestal top, $T_{i,e}^{Edge}$, are very important for the overall plasma performance under conditions of H-mode [38,39]. In particular control the ion temperature profiles in the plasma core due to its stiffness caused by the nature of turbulence due to temperature gradients[12,40]. In this section we present the results of our modelling of the pedestal characteristics for the ELM-free H-mode and compare them with experimentally found dependencies.

The pedestal radial width, Δ, changes in experiments significantly with different global and local plasma parameters. In RITM the pedestal width is defined as the distance from the separatrix to the position of the maximum ion temperature gradient. Figures 5 shows Δ normalised to the minor radius a versus the line-averaged density. The computations were done for the same heating power and Z_{eff}, by controlling the amount of impurities in the plasma through the adjustment of the erosion yield of carbon. The density has been changed by varying the intensity of external deuterium

fuelling. The decrease of Δ with density is in good correlation with the observations on DIII-D [41] explained by the hypothesis that Δ is controlled by the penetration depth of neutrals, l_n, being inversely proportional to the density. The proportionality between Δ and l_n found by RITM modelling is explicitly demonstrated in Fig.6. The penetration depth of neutrals is proportional to their velocity. Since after a charge-exchange neutrals acquire the ion temperature, one can expect that Δ should scale with . This is confirmed in Fig.7, where the dependence between Δ and is demonstrated.

In Ref. [42] it was experimentally found that the pedestal width changes proportionally to the banana orbit width $\Delta_b \approx \varepsilon^{1/2}\rho_b$, with $\varepsilon = r/R$ and ρ_b being the inverse aspect ratio and poloidal ion Larmor radius, respectively, namely, $\Delta \approx 3.3\Delta_b$. In order to check the capability of the code to reproduce these findings computations have been done by varying the plasma current I_P in the range 1.5 – 3MA. In this case both–and I_P alter in since the change of ohmic heating power and transport coefficients with the q-profile lead to a significant modification of the density and temperature profiles. Figure 8 demonstrates that our computations well reproduce the experimental results of Ref. [42]. It is, nevertheless, worthy to note that for higher plasma currents, i.e., smaller Δ_b, which are not realised in the experiment, the dependence of Δ on Δ_b becomes weaker. This result can be of importance for an extrapolation of found dependencies on reactor conditions.

In Ref. [42] the proportionality between Δ and Δ_b was considered as an argument in favour of the explanation of L-H transition through the effect of particle losses along banana orbits [43]. However, the theory [43] prescribes $\Delta \approx \Delta_b$ and the difference by the factor 3.3 is too large. Moreover, by assuming typical plasma density and ion temperature in the barrier, $5\text{-}8\times10^{13}\ cm^{-3}$ and 0.7-$1keV$, respectively, and $Z_{eff} = 2$ we find that the ion collision length is of 50-$100m$. In order to the ions would be in "banana" regime this length should be much larger than $\pi qR(R/a)^{1.5}$[44]. For JET with $q = 5$, $R = 3m$ and $a = 0.9m$ the latter value is larger than $200m$. Therefore, banana orbits can not play a significant role in the edge barrier. Finally, the RITM transport model does not include the mechanism for the formation of radial electric field due to particle losses from banana trajectories.

In concluding we bring forward a very rough qualitative explanation for the Δ scaling found in computations; a more sophisticated analysis will be done elsewhere. The formation of a pedestal occurs in the region where both DA and ITG instabilities are damped. While DA activity is strongly reduced by low collisionality and high beta, the damping of ITG turbulence requires a high enough density gradient at the edge. On the one hand, the region where such a gradient exist is determined by the neutral penetration depth and therefore $\Delta \propto \sqrt{T_i^{Edge}}/n$. On the other hand, the ion heat transport in the barrier is a neoclassical one and in all regimes decreases with increasing current due to its q-dependence [44]. Therefore, with a rising plasma current the temperature gradient increases and overcomes the stabilising effect from the density gradient at a smaller distance from the separatrix. Thus the barrier width should decrease with growing I_P. The arguments above, all together, lead to a proportionality of Δ and Δ_b.

CONCLUSIONS

The RITM code with the transport model taking into account contributions from different unstable drift modes allows a self-consistent modelling of L to H mode transition and the formation of the edge transport barrier. The transition is triggered by the reduction of the transport driven by Drift Alfven turbulence with increasing normalised plasma beta and decreasing collisionality at the edge. This allows the formation of steep density gradient at the edge due to ionisation of incoming neutrals, which suppresses the ITG instability and finally the total transport at the edge reduces to the neoclassical level.

The results of computations, done for the conditions of the selected JET discharge, show a good agreement with experiment in the value of critical power leading for the L-H transition.

A too strong puff of impurities into H-mode can destroy the pedestal and lead to the back transition to the L-mode if the radiation fraction exceeds a certain critical level (for selected conditions: $\gamma > 70\%$). It occurs as the result of the resumption of DA instability at the plasma edge caused by the radiation cooling.

Pedestal width is determined by the condition for resumption of ITG turbulence in the plasma core which is controlled both by the density and temperature profile. On the one hand, the former is determined by the penetration of neutrals and Δ scales as the velocity of charge-exchanged neutrals and varies as $\sqrt{T_i^{Edge}}$. On the other hand, the temperature scale is determined by the ion neoclassical collisionality in banana regime which decreases as $1/I_p$. All together this lead to a proportionality of the barrier width to the poloidal Larmor radius found in experiments.

ACKNOWLEDGEMENTS

Authors thank Gerard Corrigan for the help in installation and operation of the code at JET Analysed Cluster.

REFERENCES

[1]. ASDEX team, 1989, Nucl. Fusion **29** 1959

[2]. ITER Physics Expert Groups on Confinement and Transport and Confinement Modelling and Databases, ITER physics Basic Editors, 1999, Nucl. Fusion **39** 2175

[3]. JET team, 1999, Nuclear Fusion **39** 1227

[4]. Itoh K. and Itoh S.I., 1996, Plasma Phys. and Contr. Fusion **38** 1

[5]. Kim J. *et al*, 1994, Plasma Phys. and Contr. Fusion **36** A183

[6]. Rogers B.N. *et al*, 1998, Phys. Rev. Lett. **81** 4396

[7]. Kerner W., *et al*, 1998, Contrib. Plasma Phys. **38** 118

[8]. Cordey J.G., *et al*, 1998, The Scaling of the Edge Electron Temperature at the L-H Transition based on Alfven Drift-Wave Instability, Rep. JET Joint Undertaking, JET-P(98)01

[9]. Janeschitz G., *et al*, 1999, J. Nucl. Mater. **266-269** 843

[10]. Janeschitz G., *et al*, 2001, 28th EPS Conference on Contr. Fusion and Plasma Phys., Funchal, 18-21 June 2001, ECA Vol. **25A** 621
[11]. Terry P W 2000 Rev. Mod. Phys. **72**109
[12]. Baker D. R. 2001 Phys. Plasmas **8** 4128
[13]. Weiland J., 2000, Collective Modes in Inhomogeneous Plasma, Bristol: Institute of Physics Publishing
[14]. Tokar M.Z., 1994, Plasma Phys. and Contr. Fusion **36** 1819
[15]. Tokar M.Z. *et al*, 1997, Plasma Phys. Contr. Fusion **39** 569
[16]. Tokar M.Z. *et al*, 1998, Contrib. Plasma Phys. **38** 67
[17]. Carraro L.*et al*, 2000, Nucl. Fusion **40** 1983
[18]. Kalupin D. *et al.*, 2001, Plasma Phys. Contr. Fusion **43** 945
[19]. Tokar M.Z. *et al*, 2002, Plasma Phys. Contr. Fusion **44** 1903
[20]. Kalupin D. *et al*., 2003, Plasma Phys. Contr. Fusion **45** 1501
[21]. Esipchuk Yu.V *et al.,* 2003, Plasma Phys. Contr. Fusion **45** 793
[22]. Horton, W. ,1999, Rev. Mod. Phys. **71** 735
[23]. Connor J.W. and Pogutse O.P., 2001, Plasma Phys. Contr. Fusion **43** 155
[24]. Kadomtsev B.B. and Pogutse O.P., 1971, Nuclear Fusion **11** 67
[25]. Tokar M.Z. *et al*, 1999, Plasma Phys. Contr. Fusion **39** L9
[26]. Gusdar P.N., 1993, Phys. Fluids **B5** 3712
[27]. Horton, W., 1985, Plasma Phys. Contr. Fusion **27** 937
[28]. Baker D.R and Rosenbluth M.N., 1998, Phys. Plasmas **5** 2936
[29]. Hirshman S P and Sigmar D J 1981 Nucl. Fusion **21** 1079
[30]. Bateman G., *et al*, 2003, Phys. Plasmas **10** 4358
[31]. Waltz R E *et al* 1995 Phys. Plasmas **2** 2408
[32]. Tokar M.Z., 2003, Plasma Phys. Contr. Fusion **45** 1323
[33]. Diamond P.H., *et al*., 1994, Phys. Rev. Lett **72** 2565
[34]. Rognlien T.D., *et al*., 2000, Plasma Phys. Contr. Fusion **42** A217
[35]. Chankin A.V. and Saibene G., 1999, Plasma Phys. and Contr. Fusion **41** 913
[36]. Matthews G.F. *et al.*, 1999, Nuclear Fusion **39** 19
[37]. Dumortier P., *et al.*, 2002, Plasma Phys. and Contr. Fusion **44** 1845
[38]. Urano H. *et al.*, 2002, Plasma Phys. and Contr. Fusion **44** A437
[39]. JET team, 2002, Nuclear Fusion **42** 86
[40]. Ryter F., *et al.*, 2001, Phys. Rev. Lett. **86** 2325
[41]. Mahdavi M.A. *et al*, 2002, 29th EPS Conference EPS Conference on Contr. Fusion and Plasma Phys., Montreux, 17-21 June 2002,, ECA Vol. **26B** P-2.098
[42]. Hatae T. *et al*, 1998, Plasma Phys. and Contr. Fusion **40** 1073
[43]. Shaing K.C., *et al.*, 1989, Phys. Rev. Lett. **63** 2369
[44]. Balescu R 1988 Transport Processes in Plasmas (North Holland, Amsterdam) Vol.2, p.659

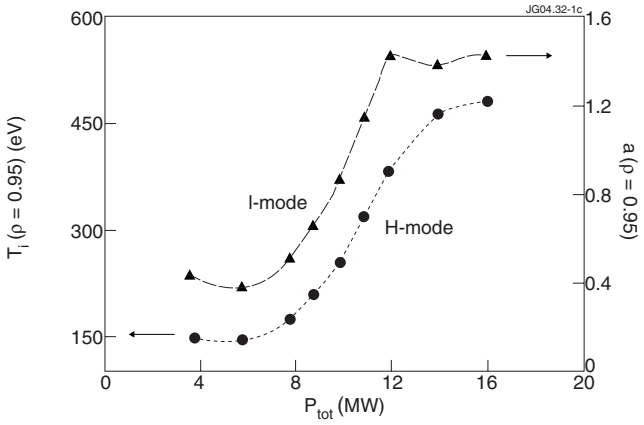

Figure 1: Normalised pressure gradient, α, and ion temperature, taken at ρ=0.95, during L-H transition.

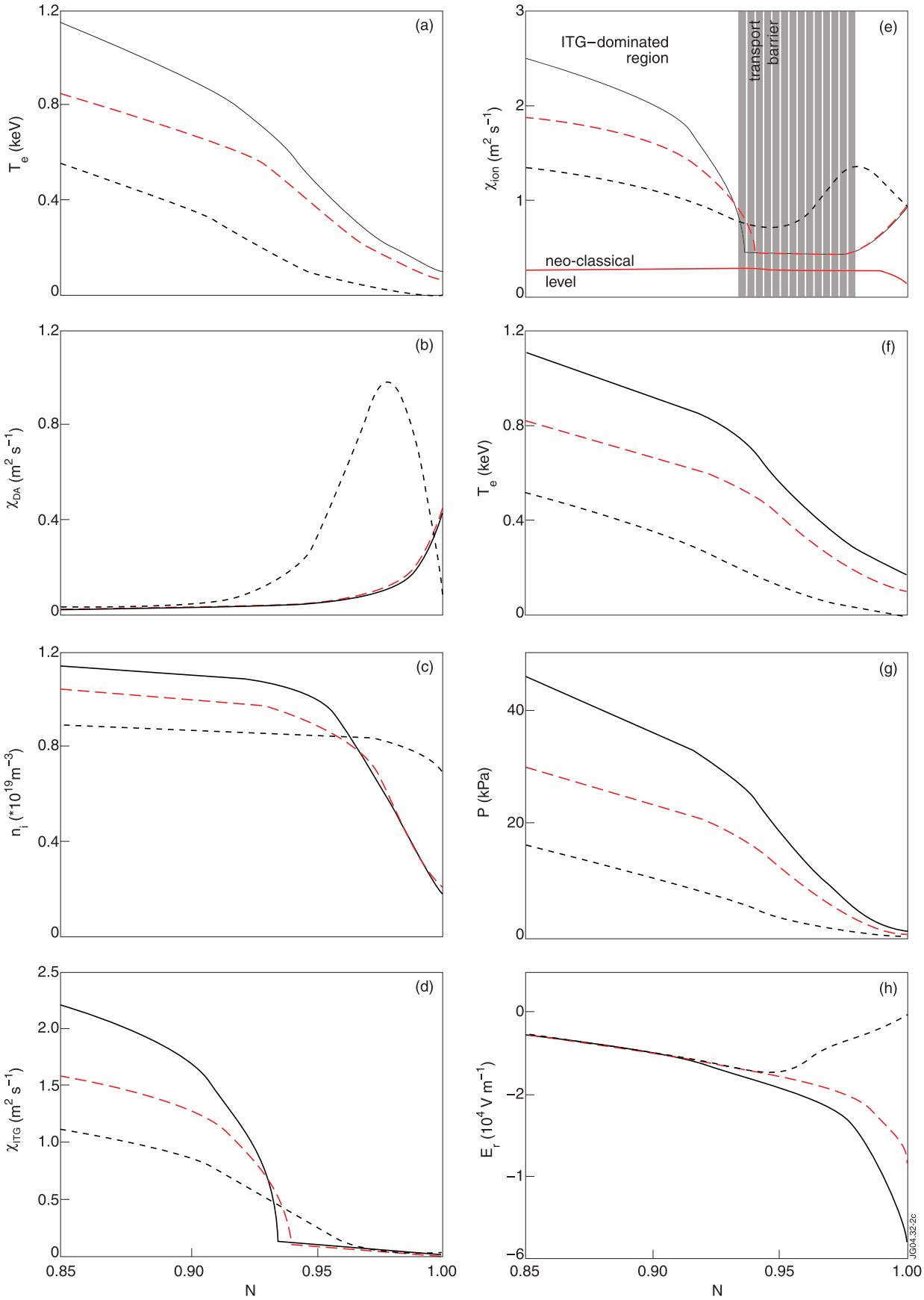

Figure 2: Radial profiles of: (a) electron temperature, (b) heat transport coefficient due to Drift Alfven instability, (c) ion density, (d) heat transport coefficient caused by ITG instability, (e) total ion heat transport coefficient, (f) ion temperature, (g) total pressure, and (h) radial electric field. (black dash – – – P_{tot}=4.2MW; red dash – – – P_{tot}=10.5MW; black solid —— P_{tot}=23.7MW).

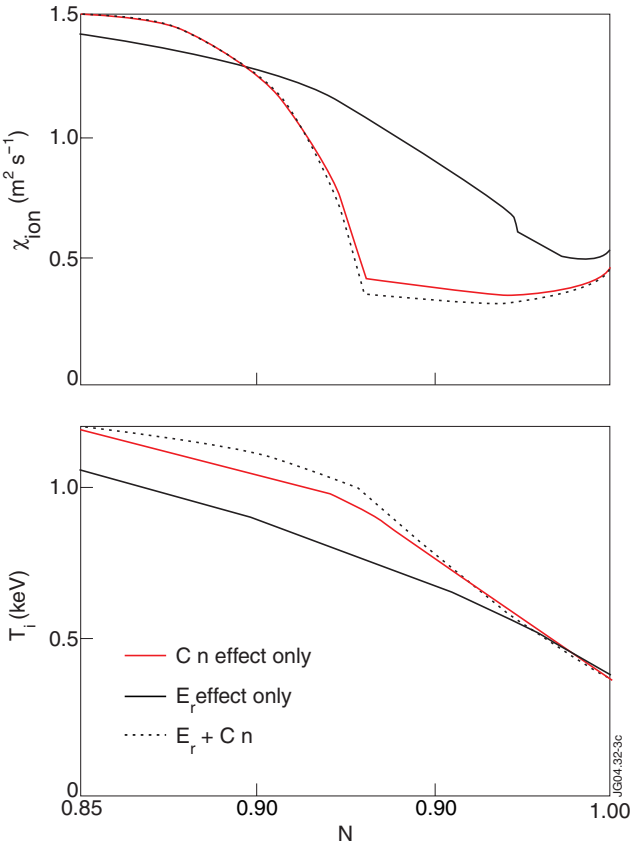

Figure 3: Ion heat conductivity and temperature obtained with different assumptions for the stabilising factors for the transport driven by ITG turbulence.

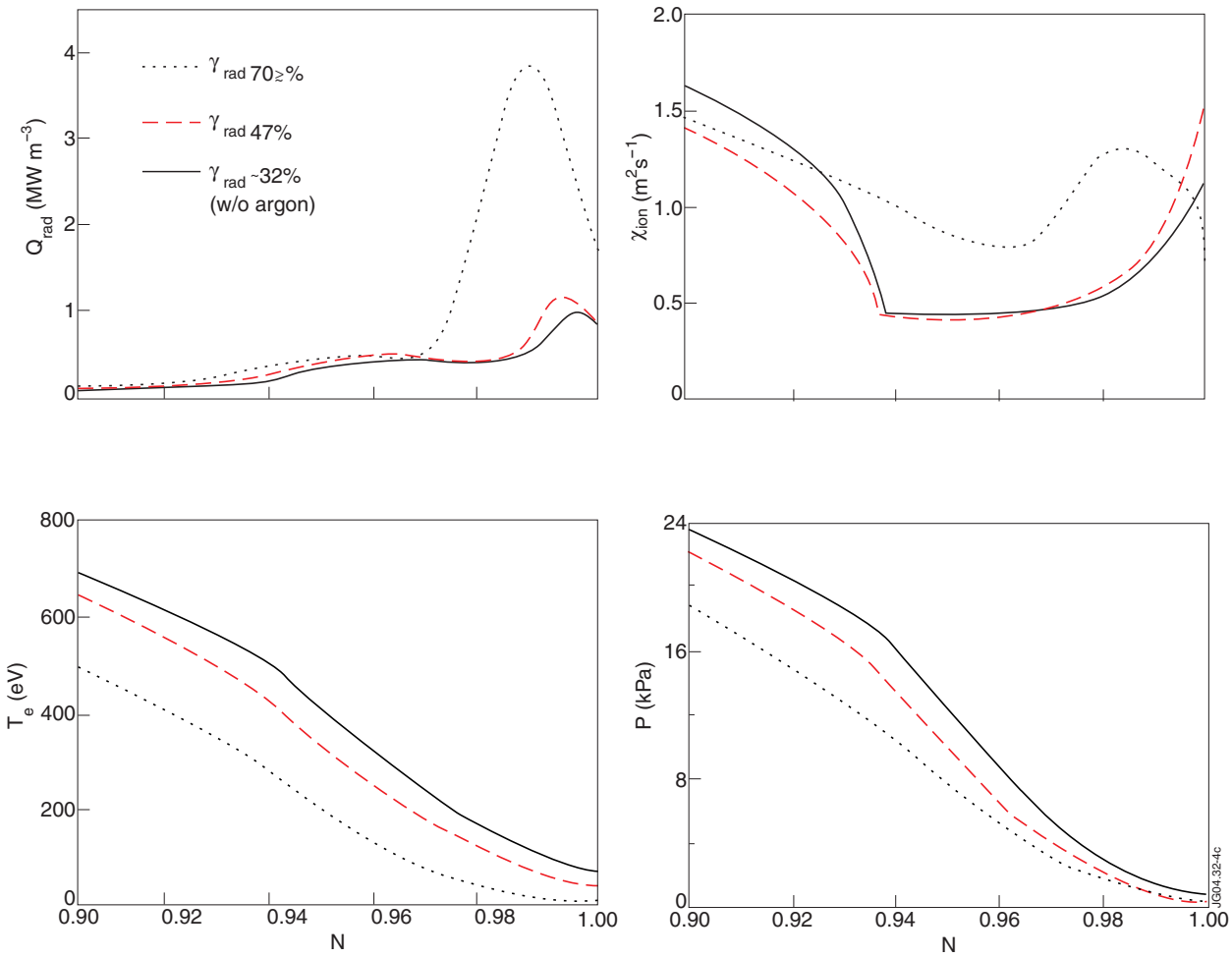

Figure 4: Radial profiles of radiation power density, electron temperature, ion heat transport coefficient and total pressure computed with different intensity of argon impurity injection.

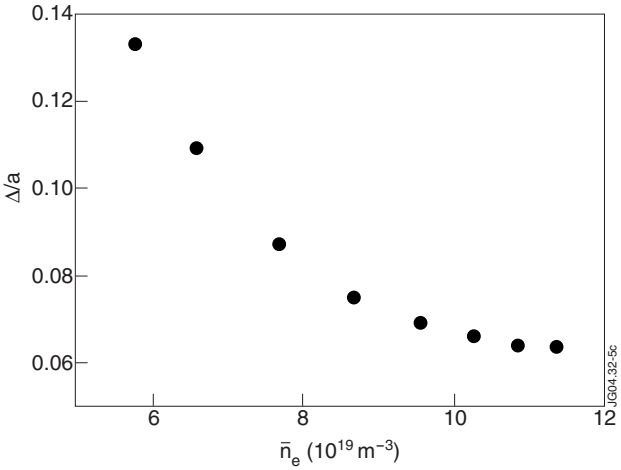

Figure 5: Pedestal width normalised to the plasma minor radius as a function of the line-averaged density.

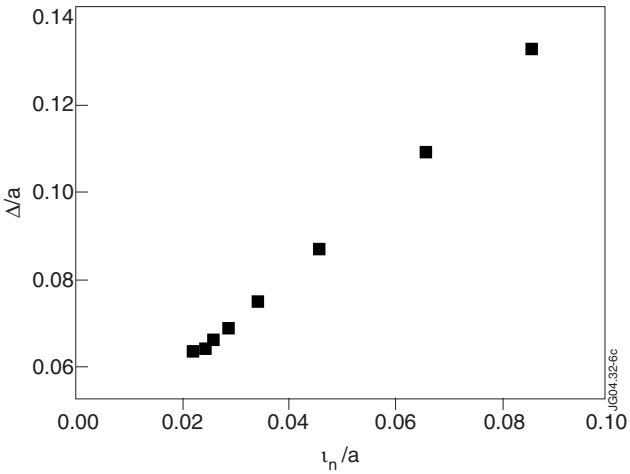

Figure 6: Normalised pedestal width as a function of normalised neutral penetration depth.

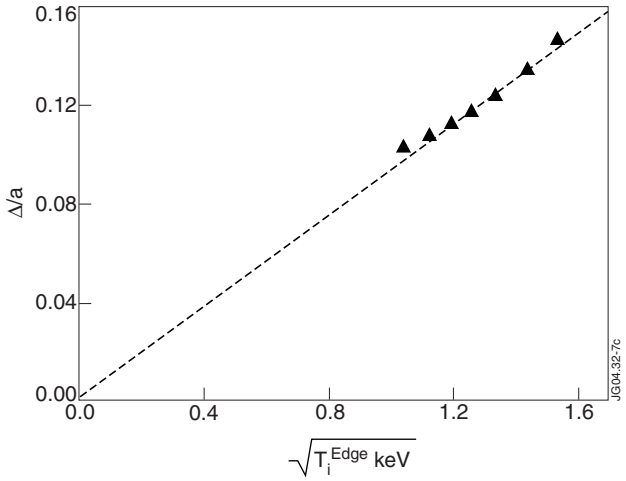

Figure 7: Normalised pedestal width as a function of ion temperature at the top of pedestal.

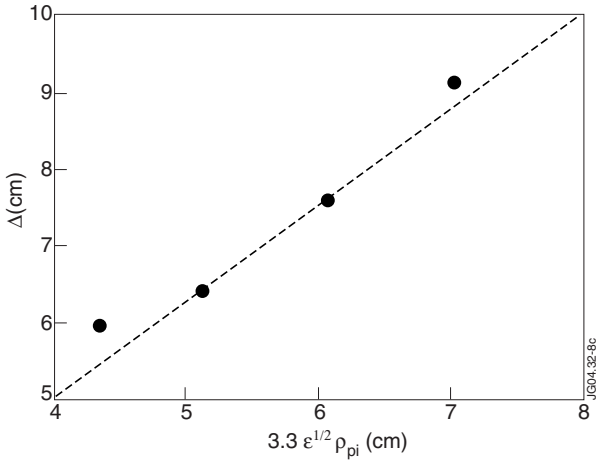

Figure 8:Pedestal width as a function of the banana orbit width (the dashed line represents the dependence $\Delta = 4.125^{*}\ \varepsilon^{1/2}\ \rho_{Pi}$).